# Impact of Process Poisons on the Performance of Post-Phthalate Supported Ziegler–Natta Catalysts in Gas Phase Propylene Polymerization

Abdulrahman Albeladi, Akhlaq Moman, Timothy F L Mckenna

# Impact of Process Poisons on the Performance of Post-Phthalate Supported Ziegler Natta Catalysts in Gas Phase Propylene Polymerization

*Abdulrahman Albeladi,[1] Akhlaq Moman,[2] Timothy F. L. McKenna[1,*]*

Catalysis, Polymerization, Processes, and Materials (CP2M), UMR 5128 CNRS/UCBL/CPE-Lyon, 69616 Villeurbanne Cedex

[2]SABIC Technology Center Riyadh, 2nd Industrial Area, Kharj Highway,Riyadh, 11422, Saudi Arabia

*timothy.mckenna@univ-lyon1.fr

## Abstract

The impact of common process catalyst poisons on the performance of a 6th generation Ziegler Natta catalysts during the gas phase polymerization of propylene were examined using two approaches: introducing propylene without purification, or with one or two sets of purification columns, and by introducing carbon dioxide ($CO_2$), oxygen ($O_2$), water ($H_2O$), methanol ($CH_3OH$), ethyl acetate ($C_4H_8O_2$), and dimethyl sulfoxide ($C_2H_6SO$) during the polymerization. As expected, purification columns increass the catalyst activity significantly, slightly reduce catalyst decay. Injecting TiBA during the reaction leads to an activity increase. The addition of two full sets of columns substantially increased the repeatability of polymerization reactions. The power of deactivation of poisons injected during the polymerization reaction was: $O_2$ > $CO_2$ > $CH_3OH$ > $C_2H_6SO$ > $C_4H_8O_2$ > $H_2O$. Adding $CO_2$, $O_2$, and $CH_3OH$ resulted in a progressive decrease in molecular weight while almost no effect was observed with $H_2O$. However, $C_4H_8O_2$, and $C_2H_6SO$ resulted in a mild increase in molecular weight. Additionally, the effects on crystallinity and stereoregularity were similar where $CO_2$, $O_2$, $H_2O$, and $CH_3OH$ caused a progressive decrease while $C_4H_8O_2$, and $C_2H_6SO$ resulted in a mild increase, indicating some isotacticity control by these two poisons.

**Keywords**: ziegler natta catalysts, gas phase polymerization, feed poisons, polypropylene, post phthalate Catalysts.

## 1. Introduction

Polypropylene is a thermoplastic polymer that is used in a wide range of applications from household articles, food, and packaging applications, to the medical and performance engineering applications. Most of the polypropylene currently in the market is produced using Ziegler-Natta coordination catalysts. Process technologies for propylene polymerization are mainly categorized by the phase of the reaction: gas, slurry, and bulk or a combination thereof. Gas phase processes constitute a major volume in the market due to their relatively cheaper cost of operation and the robustness of the overall process. However, these processes are more prone to instabilities that could lead to problems as small as a slowdown in the process or as catastrophic as a complete agglomeration of the polymer powders inside the reactor. One of the most crucial quality parameters for the process and product reliability and good performance is the quality of the feed, specifically, the monomer, propylene. Due to the high sensitivity of Ziegler-Natta catalysts to polar compounds, extensive purification is often employed in all polymerization processes to avoid any instabilities in production or in the product quality. Though it is a well-known fact that these catalysts are sensitive to impurities, there are not many studies that quantified the impact of some common poisons on the catalyst activity for the latest supported Ziegler Natta generations in gas phase polymerizations, nor investigated the consequences on the polymer microstructure and powder morphology, though such studies are currently of more interest due to the growing interest in monomers produced via chemical recycling of plastics which would contain more contaminants in comparison to conventionally produced monomers. [1–3] In this introduction, we will take a brief look at the few publications that have investigated the effects of poisons on propylene polymerizations experimentally and theoretically.

Yuan et al. [4] studied the effect of isobutyl alcohol, phenol, and trichloroacetic acid on the catalyst activity of a second generation Ziegler Natta system in slurry

polymerization for polypropylene. They added their poisons 25 minutes prior to starting the reaction. Both the alcohol and the phenol led to an enhancement of activity in the presence of hydrogen and no or a mild increase in the absence of hydrogen. They postulated that the frequent transfer to hydrogen leads to favorable interactions between the hydrogen and the additive molecules; isobutyl alcohol and phenol. However, this was not the case with the acid which decreased activity significantly. They also investigated the effects on the polymer microstructure and found that the alcohol reduces the polymer tacticity and to a milder degree the molecular weight. With the phenol, the only effect was a noticeable decrease in molecular weight. The trichloroacetic acid did not affect tacticity, but a clear broadening in the MWD was observed.

Vizen et al. [5] used carbon disulphide ($CS_2$) which is a known catalyst poison in an attempt to discriminate between hydrogen activated sites and sites at the beginning of the reaction. They used a fourth generation PP ZN catalyst in slurry polymerization reaction where $CS_2$ is added for most experiments after the beginning of the reaction. They showed that $CS_2$ poisons the catalyst active sites similarly in the presence and absence of hydrogen. One interesting observation was that the poison deactivates the isotactic sites to a higher degree relative to the non-specific sites but without any decrease in isotacticity and an increase in some experiments. Moreover, a noticeable decrease in the weight average molecular weight is observed while the number average molecular weight decreased to a lesser degree which led to mild narrowing in the molecular weight distribution.

Tangjituabun et al. [6] used a third generation Ziegler Natta catalyst to test the effects of methanol, acetone, and ethyl acetate, in a slurry stopped flow reaction setup for propylene polymerization. They treated the catalyst with the poisons in a molar ratio to Ti of around 0.1 for one minute before starting the reaction. The highest drop in activity was noticed with methanol followed by acetone and finally ethyl acetate. They explain the strong effect of methanol with a reaction forming titanium chloride alkoxides which are inactive for polymerization. They have shown as well that the deactivation effect of methanol is due to the decrease in the active sites concentration while both the reaction with and without methanol had similar propagation constants. They checked the stereoregularity of the polymers using $^{13}C$ NMR and did not observe any effects.

Arjmand et al. [7] have introduced water and carbonyl sulfide in the propylene feed at different concentrations to investigate the effects on some polymer properties of polypropylene using a commercial Ziegler Natta catalyst. They did not investigate the effect of these two poisons on activity, but rather focused on the microstructural properties of the resulting polymers. Their results show a trend of narrowing molecular weight distribution with both poisons and a decrease in the isotactic pentads as well. Another relevant observation was the decrease in crystallinity which they have attributed to the drop in isotacticity. They have also reported an increased transparency of the films of their polymers due to the reduction in surface irregularities and the increased atacticity.

In this study, we will be reporting the effects of the monomer (i.e., propylene) purification system and reaction temperature on the catalyst activity and decay. Moreover, we will systematically investigate the impact of the following known catalyst poisons: carbon dioxide ($CO_2$), oxygen ($O_2$), water ($H_2O$), methanol ($CH_3OH$), ethyl acetate ($C_4H_8O_2$), and dimethyl sulfoxide ($C_2H_6SO$), on the catalyst activity and decay, the polymer microstructure (i.e., molecular weight, stereoregularity, crystallinity), and powder morphology. Additionally, we will discuss the effects of said poisons on the reactor fouling and operability. The study is conducted on a sixth generation (post-phthalate) Ziegler-Natta polypropylene catalyst in a gas phase semi-batch polymerization reactor. The selected poisons have been chosen to satisfy the following criteria as much as possible: commonly present poisons in propylene, different functionalities, and the ability to safely handle them within the experimentation facility.

## 2. Experimental

### 2.1. Materials

The catalysts used in this study are sixth generation (phthalate free) Ziegler Natta catalysts developed by SABIC, referred to as ZN-1, and ZN-3. Both catalysts have comparable titanium contents of around 3 wt%, ZN-1 is composed of N,N-dimethyl benzamide and 9,9-bis(methoxymethyl)fluorene as internal donors, while N,N-dimethyl

benzamide, and Iso-propyl-iso-pentyl dimethoxypropane were used for ZN-3. Triethylaluminum (TEA) and triisobutylaluminum (TiBA) were purchased from Witco, and diluted to approximately 1 M in n-heptane which was purified using Mbraun solvent purification unit. The external electron donor: diisopropyldimethoxysilane (P-Donor) was purchased from ABCR and stored over molecular sieves. Ethyl acetate, methanol, and dimethyl sulfoxide were purchased from Sigma Aldrich and bubbled using argon for1 hour before use to remove free oxygen. Distilled and demineralized water was acquired from a water purification unit in the laboratory. Propylene, oxygen, and carbon dioxide were purchased from Air Liquide.

### 2.2. Polymerization Setup and Procedure

The polymerization experiments are conducted in a 2.5 L semi-batch reactor in gas phase. The setup schematic is shown in **Figure 1** with each component numbered, the numbering details are shown in **Table 1**. Propylene is sent from the cylinder to the reactor passing through two sets of purification columns, each set contains a copper oxide bed, a mixture of molecular sieves (i.e., 13X, 3A) bed, and a Selexorb bed. The flow is monitored and recorded every 10 seconds through a mass flow meter connected to a data acquisition computer. The reactor is operated under isothermal conditions, the heating/cooling water bath maintains the internal temperature of the bath at a set point. The other major components are the vacuum pump, and the poisons feeding system. The poisons feeding system has been fabricated in-house which is mainly a 50 ml steel cartridge in a conical shape supplied with one side inlet connected to three lines: vacuum, argon, and propylene. The cartridge is isolated by two valves at the top and the bottom, the top valve is used to inject the liquid poisons under argon. In the case of the gaseous poisons, another fixed volume tube with two isolation valves is connected, this tube is connected directly to the gaseous poison cylinder.

The polymerization procedure starts by drying the reactor under vacuum at a temperature around 90 °C for one hour followed by five cycles of argon flushes and vacuum. Afterwards, the reactor is cooled down to below 35 °C for the injection of the reaction modifiers. The external electron donor is injected first using a syringe feeding into

the reactor injection port under argon followed by the co-catalyst in the same manner. Both the external electron donor and the co-catalyst are prepared beforehand in clean and dried Schlenks. In the case of the external electron donor, the neat material is stored over molecular sieves in the glove box. The catalyst is added to a 60 ml steel cartridge that is stored in an over at around 90 °C before being introduced to the glove box where the catalyst (50 mg) is mixed with a specific amount of salt (NaCl) which acts as a seedbed, the amount of salt is 20 g for all the experiments described in this chapter. The cartridge is isolated in the glove box and then mounted on the reactor where the two external connections are vacuumed for 15 minutes to remove air. After the injection step of modifiers described previously, the required amount of hydrogen is introduced and then, the reactor is heated to the reaction temperature and mixing is started at 250 rpm. Once the reaction temperature is approached, the catalyst is injected by introducing propylene from the pressure reducer by-pass line, the cartridge is pressurized and then released into the reactor, this pressure injection is repeated for 15 times to ensure complete flushing of the cartridge's content into the reactor. Afterwards, the same by-pass line is opened to pressurize the reactor to 0.1 barg above the pressure reducer set point, this line is isolated immediately after the desired pressure is reached and the flow is diverted to the pressure control line where propylene keeps flowing as the pressure reduces in the reactor below the pressure control valve set point. The steps that follow are for the preparation of the poisons system and injection. The same port used to inject the catalyst is connected to the poisons cartridge which then undergoes 10 cycles of argon-vacuum purges. For the liquid poisons, they are injected in the steel cartridge at the top under argon and then the cartridge is heated to vaporize the liquid, at 12 minutes after the reaction start, propylene is diverted using a three-way valve to flow through the poisons cylinder for injection. For the gaseous poisons, the desired amount is calculated based on the pressure of the cylinder and the volume of the injection tube and then injected similarly but at minute 8 after reaction. The reactor pressure and temperature data are collected every minute for the duration of the reaction which is 60 minutes after which the reactor is cooled down and vented. The collected polymer is washed with water to dissolve the salt and dried in a vacuum oven at 80 °C for two hours.

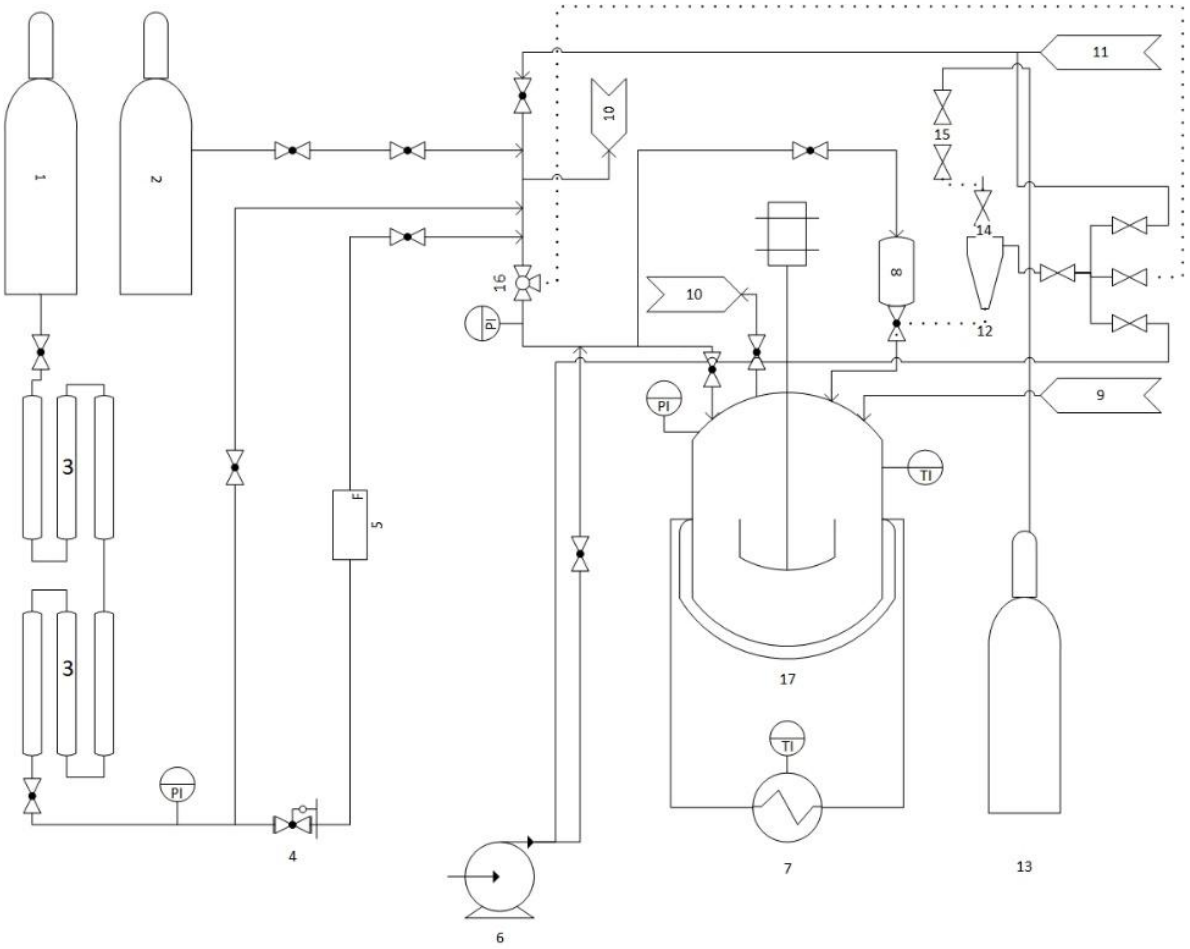


***Figure 1****. Gas phase propylene polymerization setup.*

***Table 1****. Description of the reaction setup components numbering shown in Figure 1.*

| | |
|---|---|
| 1. Propylene cylinder | 9. Injection port |
| 2. Hydrogen cylinder | 10. Vent streams |
| 3. Purification columns | 11. Argon |
| 4. Pressure control valve | 12. Poison's injection cylinder |
| 5. Mass flow meter | 13. Gaseous poisons cylinders |
| 6. Vacuum pump | 14. Injection port of poisons |
| 7. Heating/cooling bath | 15. Gaseous poisons injection tube |
| 8. Catalyst injection cylinder | 16. Three-way valve for propylene feed |
| | 17. 2.5 L spherical reactor |

## 2.3. Polymer Characterization

We would like to emphasize the fact that the characterized polymers from all the poisons experiments are affected by the dilution effect of the polymers produced in the

period before injecting the poison which ranges from 30% to 70% of the total polymer yield depending on the reaction. This may lead to an underestimation or masking of the real response when the poisons are added in regard to the polymer microstructure and morphology characteristics especially in the experiments where activity is near zero after the addition of the poison.

### 2.3.1. Gel Permeation Chromatography (GPC)

Molecular weight parameters (number average molecular weight ($M_n$), weight average molecular weight ($M_w$), molecular weight distribution (MWD), and the z and z+1 average molecular weight) were measured using a GPC. The analysis was carried out in a Polymer Labs HT GPC 220 equipped with a differential refractive index detector. Data acquisition was done using Polymer Labs Cirrus GPC software. A sample of 30 mg of the polymer is dissolved in BHT stabilized 1,2,4-trichlorobenzene (TCB) and analyzed at 160 °C.

### 2.3.2. Differential Scanning Calorimetry (DSC)

A Mettler Toledo DSC 1 system was used to analyze crystallization, the DSC is equipped with an auto-sampler and a 120 thermocouple sensor. All samples were accurately weighed (5 ± 0.1 mg) and sealed in aluminium pans of volume 40 μL. Samples were heated to 200 °C to erase thermal history and then cooled to −20 °C before being heated again to 200 °C at a rate of 10 °C per minute. The melting enthalpy for a 100% crystalline PP of 209 $J.g^{-1}$ was used to compute the crystallinity fractions of the samples. [8]

### 2.3.3. Crystallization Elution Fractionation (CEF)

Crystallization Elution Fractionation (CEF) from Polymer Char was used to analyze the tacticity of polypropylene. Around 4 mg of polymer was added into a 10 ml vial and placed in the autosampler which automatically adds around 8.0 mL of BHT stabilized 1,2,4-trichlorobenzene (TCB). The analyses started by heating the dissolved sample to 160°C for an hour, after which the sample was maintained at 140°C for 20 minutes. The polymer solution was then pumped through the CEF column while being cooled to 35°C at a cooling rate of 2.0 °C per min and crystallization flow rate of 0.0065 mL/min. After the sample was

completely deposited in the CEF column, the elution cycle stared with a heating rate of 4.0°C/min to 140°C and an elution flow rate of 1.0 mL/min.

### 2.3.4. Powder Morphology Analyses

The performed powder morphology analyses in this work are the bulk density measurement, and the particle size distribution. The bulk density is conducted by filling a recipient of a specific known volume with the powder and measuring the weight of the sample. The weight of the powder divided by the known volume of the recipient gives what is called the resin settled bulk density. The particle size distribution and analysis of the powder were performed in a Malvern Mastersizer 3000 particle analyzer equipped with a dry powder disperser (Aero S).

## 2.4. Experiments

For this study, two main experimental programs were conducted; the first was to check the effect of purification columns on the catalyst kinetic response and activity at different operating temperatures, and the second one was to study the impact of select poisons by systematic additions on the catalyst kinetic response, polymer properties, powder morphology, and reactor stability.

The two variables in the first program presented in **Table 2** are the purification columns, and the reaction temperature. Three temperatures were tested for the three variations in purification columns; in the first set of experiments, no purification columns were used (NC) with propylene directly fed from the cylinder to the reactor, one purification column set was used in the second experimental set, and finally two sets of columns for the final experimental set. ZN-3 catalyst was used to perform this experimental program with triethylaluminium as a co-catalyst with a propylene pressure of 6.0 barg, no external electron donor nor hydrogen were introduced. Additionally, the set of experiments from 10 to 13 are designed to investigate the same effect but using another co-catalyst, TiBA, but with an additional dimension of study which is the additional injections of TiBA in experiment 11 while no propylene purification is being used.

***Table 2**. Experimental reaction conditions for the purification columns set.*

| SN | Purification Columns | Co-catalyst | Al/Ti (Doses) | ED | $H_2$ (mol%) | P (barg) | T (°C) |
|---|---|---|---|---|---|---|---|
| 1 | No columns (NC) | TEA | 52 | No ED | 0.0 | 6.0 | 56 |
| 2 | No columns (NC) | | | | | | 76 |
| 3 | No columns (NC) | | | | | | 94 |
| 4 | One set (1SC) | | | | | | 56 |
| 5 | One set (1SC) | | | | | | 76 |
| 6 | One set (1SC) | | | | | | 94 |
| 7 | Two sets (2SC) | | | | | | 56 |
| 8 | Two sets (2SC) | | | | | | 76 |
| 9 | Two sets (2SC) | | | | | | 94 |
| 10 | No columns (NC) | TiBA | 52 | No ED | 0.0 | 6.0 | 76 |
| 11 | No columns (NC) | | 52 (2) | | | | |
| 12 | One set (1SC) | | 52 | | | | |
| 13 | Two sets (2SC) | | 52 | | | | |

***Table 3**. Experimental reaction conditions for the poisons addition experiments.*

| SN | Co-catalyst | Al/Ti (doses) | ED | Si/Ti | $H_2$ (mol%) | P (barg) | T (°C) | Poison | Poison Concentration (ppmw) |
|---|---|---|---|---|---|---|---|---|---|
| 14 | TiBA | 54 (1) | P | 1.6 | 2.1 | 7.0 | 69 | None | 0.0 |
| 15 | | 54 (2) | | | | | | None | 0.0 |
| 16 | | 54 (1) | | | | | | $CO_2$ | 2.9 |
| 17 | | 54 (1) | | | | | | $CO_2$ | 8.7 |
| 18 | | 54 (1) | | | | | | $CO_2$ | 14.4 |
| 19 | | 54 (1) | | | | | | $CO_2$ | 20.2 |
| 20 | | 54 (3) | | | | | | $CO_2$ | 40.4 |
| 21 | | 54 (1) | | | | | | $O_2$ | 1.7 |
| 22 | | 54 (1) | | | | | | $O_2$ | 3.4 |
| 23 | | 54 (1) | | | | | | $O_2$ | 5.0 |
| 24 | | 54 (1) | | | | | | $O_2$ | 8.0 |
| 25 | | 54 (3) | | | | | | $O_2$ | 16.0 |
| 26 | | 54 (1) | | | | | | $H_2O$ | 1000.0 |
| 27 | | 54 (1) | | | | | | $H_2O$ | 2000.0 |
| 28 | | 54 (3) | | | | | | $H_2O$ | 4000.0 |
| 29 | | 54 (1) | | | | | | $CH_3OH$ | 40.0 |
| 30 | | 54 (1) | | | | | | $CH_3OH$ | 80.0 |
| 31 | | 54 (1) | | | | | | $CH_3OH$ | 633.0 |
| 32 | | 54 (3) | | | | | | $CH_3OH$ | 1200.0 |
| 33 | | 54 (1) | | | | | | $C_4H_8O_2$ | 155.0 |
| 34 | | 54 (1) | | | | | | $C_4H_8O_2$ | 310.0 |
| 35 | | 54 (1) | | | | | | $C_4H_8O_2$ | 620.0 |
| 36 | | 54 (3) | | | | | | $C_4H_8O_2$ | 1200.0 |
| 37 | | 54 (1) | | | | | | $C_2H_6SO$ | 64.0 |

| | | | | | |
|---|---|---|---|---|---|
| 38 | | 54 (1) | | $C_2H_6SO$ | 128.0 |
| 39 | | 54 (1) | | $C_2H_6SO$ | 320.0 |
| 40 | | 54 (3) | | $C_2H_6SO$ | 640.0 |

In the second experimental program shown in **Table 3**, six catalyst poisons have been injected: Carbon Dioxide ($CO_2$), Oxygen ($O_2$), Water ($H_2O$), Methanol ($CH_3OH$), Ethyl Acetate ($C_4H_8O_2$), and Dimethyl Sulfoxide ($C_2H_6SO$), at varying concentrations. This set of experiments was performed using ZN-1 catalyst with triisobutylaluminum (TiBA) as a co-catalyst, and diisopropyl dimethoxysilane (P-Donor) as an external electron donor, at a reaction temperature and pressure of 69 °C, and 7 barg, respectively. Hydrogen was used as a chain transfer agent at a concentration of 2.1 mol%, and a Si/Ti molar ratio of 1.6 was used. For the reference and each poison, one more additional experiment was conducted where one additional injection of the co-catalyst was administered for the reference, and two for the poisons' experiments, to study the possibility of recovering catalyst activity by reactivating the poisoned catalytic sites.

## 3. Results and Discussions

### 3.1. Reaction Rates and Decay

#### 3.1.1. Effect of Purification and Temperature

The propylene used for our experiments is grade N25 purity supplied by Air Liquide. Estimates of the impurities in the bottle are shown in **Table 4** as received from the supplier. The standard commercial preferred purity for propylene used in polymerization reactors are also presented in the same table. As we have explained earlier in the experimental part, we use two sets of purification columns, each set contains three different columns as shown in **Figure 2** along with the contaminants removed in each stage.

***Table 4****. Propylene N25 specifications and standard commercial PP plants specification.*

| Impurity | Concentration (ppm mol) | Commercial Specifications (ppm mol)[1] |
|---|---|---|

[1] Internal SABIC standards.

| | | |
|---|---|---|
| **$H_2O$** | < 25 | < 0.1 |
| **$O_2$** | < 10 | < 0.05 |
| **$CO_2$** | < 5 | < 0.1 |
| **$N_2$** | < 200 | 0.5 |
| **$H_2$** | < 10 | 0.1 |
| **Total Sulfur** | < 2 | < 0.1 |
| **Total alkanes** | < 5000 | 1000 |
| **Total Alkenes** | < 20 | 2.0 |

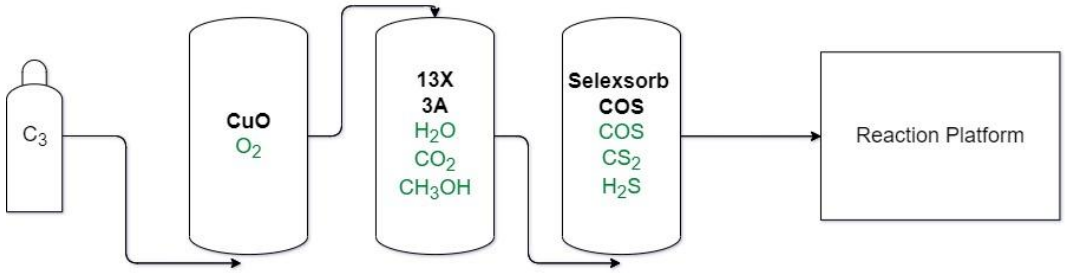


***Figure 2**. Lab purification setup for Propylene.*

It is well known that polar chemical compounds such as those present as impurities in the propylene used here are strong poisons for Ziegler Natta catalysts. Hence, most well controlled experimental setups on the industrial scale are equipped with purification systems for the monomers to guarantee the maximum possible purity. However, the effect of using purification columns in lab scale reactors is not well investigated in terms of its impact on activity and decay. Looking at **Figure 4-A**, at the lowest reaction temperature, we can see the net activity tripling when adding one set of columns. Adding an extra set of columns further increases activity by around 30% for the same temperature. The difference is sustained to a lesser degree when increasing the reaction temperature to 76 °C. However, for the highest temperature, 94 °C, this significant difference in net activity diminishes almost completely. We believe this is due to the innate self-extinguishing property of this catalyst system in which the active sites become deactivated at temperatures higher than the normal industrial operating temperatures. We have no evidence to further understand the mechanism by which such deactivation is taking place but based on these experiments which are purposefully designed to eliminate as many variables as possible, it could be either of thermal origin, or an interaction of the co-catalyst with the internal donors of the catalyst becoming more pronounced as temperature increases. Moreover, in the same graph we can see a similar difference in activity when

using TiBA as a co-catalyst with an overall higher productivity as compared to when TEA is used.

Graphs A, B, and D in **Figure 3** show the reaction rate curves for the following reaction temperatures respectively when using TEA as a co-catalyst: 56 °C, 76 °C, and 94 °C, while graph C shows the reaction rates when using TiBA as a co-catalyst at 76 °C, all the profiles follow the classical decay type reaction rate progression with time with no significant visible differences in decay. The additional injection of TiBA shown in graph C led to an increase in the reaction rate which is most likely due to scavenging some of the impurities present in the reactor and reactivation of catalyst sites.

Moreover, if we calculate a simple decay index which is dividing the maximum rate by the final rate and plot the values as a function of reaction temperature as shown in **Figure 4-B**, we can observe a clear increase of decay as the temperature rises when no purification is used. Nonetheless, the difference in decay between the low and highest temperatures increases significantly in absence of purification columns, this hints to the point that the decaying activity with temperature is not only a thermal deactivation phenomenon but impurities can also play a role there as well. Moreover, the decay reduces when purification columns are added which shows the effect of impurities in propylene on the time dependant deactivation. Moreover, this effect is more pronounced at the highest reaction temperature, which could be due to either higher reactivity of the impurities present in the feed or higher mobility of poisons at elevated temperatures leading to the increase in decay over reaction time. Finally, there is no change in the decay indices with different purification settings when we use TiBA as a co-catalyst.

Another important observation we have seen was the effect of number of purification columns sets on the repeatability of experiments. Repeatability is a serious challenge in Ziegler Natta polymerization experiments that is usually exacerbated in gas phase. There are many factors that influence this, but the main fundamental fact is that such catalysts are highly sensitive to all kinds of impurities which poses this challenge. One can be extremely careful in terms of operational accuracy but would still end up with an unsatisfactory repeatability. We noticed a significant improvement in experimental

repeatability after the addition of a second set of columns. **Table 5** shows the productivities of five replicates of experiments number 4 and 7. When we compute the relative standard deviation (RSD) for both sets of experiments, we have a significant drop from ca. 7% to ca. 1%. These results show the importance of monomer purity in obtaining repeatable results which eventually saves a lot of time and effort for researchers and ensures better quality of results.

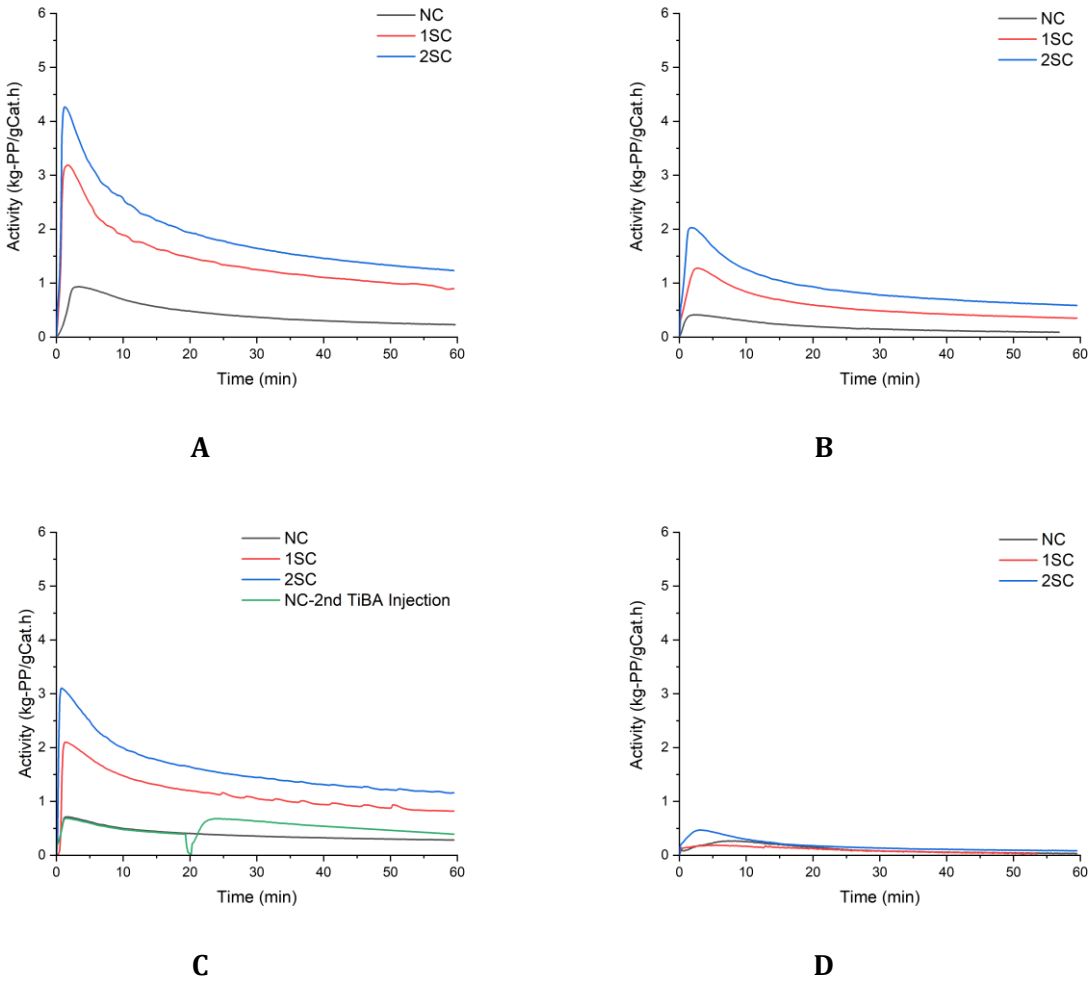


***Figure 3****. The effect of using purification columns on the catalyst activity in propylene polymerization;* ***A****. at 56 °C,* ***B****. at 76 °C,* ***C****. at 76 °C with TiBA, and* ***D****. at 94 °C.*

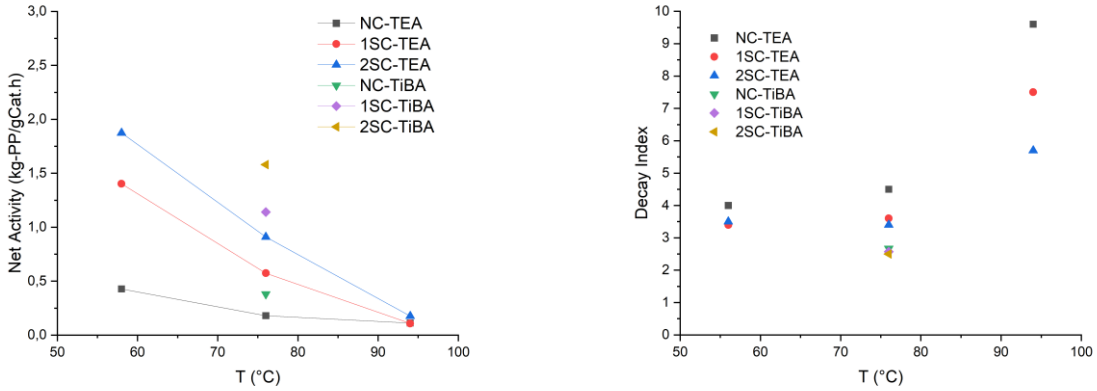


**A** **B**

***Figure 4****. A. Net activities, and B. decay indices, plotted against reaction temperature.*

***Table 5****. Activities of replicate experiments with one and two sets of purification columns.*

| **Experiments** | **Activity (kg-PP/gCat.h)** | |
|---|---|---|
| | **One Set of Columns** | **Two Sets of Columns** |
| **Replicate 1** | 1.40 | 1.87 |
| **Replicate 2** | 1.33 | 1.85 |
| **Replicate 3** | 1.53 | 1.89 |
| **Replicate 4** | 1.37 | 1.84 |
| **Replicate 5** | 1.56 | 1.86 |

### 3.1.2. Systematic Addition of Poisons

Quantification of the depressive effect of catalyst poisons on its activity and decay is of important industrial utility as it sets many process design limits and informs the operability and handing of polymerization processes. The methodology we have adapted is to inject the poison after the reaction has started allows us to see how the reaction rate changes, and also to ensure the repeatability of experiments as all experiments have the same conditions for the period before poisons' injection. The reaction rates of the reference experiment (i.e., 14) and experiment 15 in which TiBA is injected after 35 minutes of reaction are shown in **Figure 5**. Both experiments show the same profile with two characteristic regions of decay, the first one exhibiting fast decay from the time of catalyst injection until around 10 minutes after which follows a period of milder decay. We have

added the second injection of the co-catalyst in order to understand its impact on the catalyst without the presence of poisons, as we have utilized this methodology for all the used poisons in order to investigate any possible reactivation by the co-catalyst, further decay in the catalyst activity is observed after this injection which is due to the over reduction in Ti oxidation state. [9, 10]

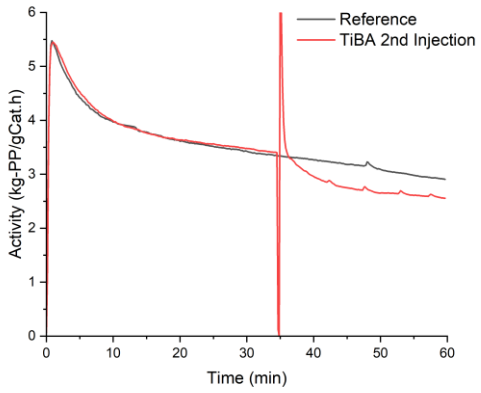


***Figure 5**. Catalyst activity rate for the reference experiment for the poisons experiments set and the reference with the additional TiBA injection at 35 min post reaction start.*

The effect of $CO_2$ injection at different concentrations is demonstrated in **Figure 6-A**, all the reactions show remarkably high repeatability in the first 8 minutes, the RSD is within 1.0%. At the lowest concentration of $CO_2$, the activity is reduced by around 40% and the kinetic profile shows significant progressive decay compared to the reference profile. For the next higher concentrations of $CO_2$, the kinetic profile shows a different behavior of decay which is characterized by an exponential decay for a few minutes followed by a period of stability. The stability period is followed by a recovery period in which we observe the reaction rate starts to slowly increase. This behavior shows that poisoning by $CO_2$ is reversible. This reactivation behavior of the catalyst is most clear in the experiment where two additional TiBA injections are added. We can see a very mild recovery of activity after the first shot around minute 20 that is further increased at minute 30 after the second shot where the reaction rate continues to recover until eventually reaching a similar activity of experiment 17 even though the $CO_2$ concentration in this experiment is five times higher than the former experiment. The productivities as a function of poison

concentration are fitted using a first order exponential decay equation with an adjusted coefficient of determination ($R^2$) around 0.97 as shown in **Figure 6-B**.

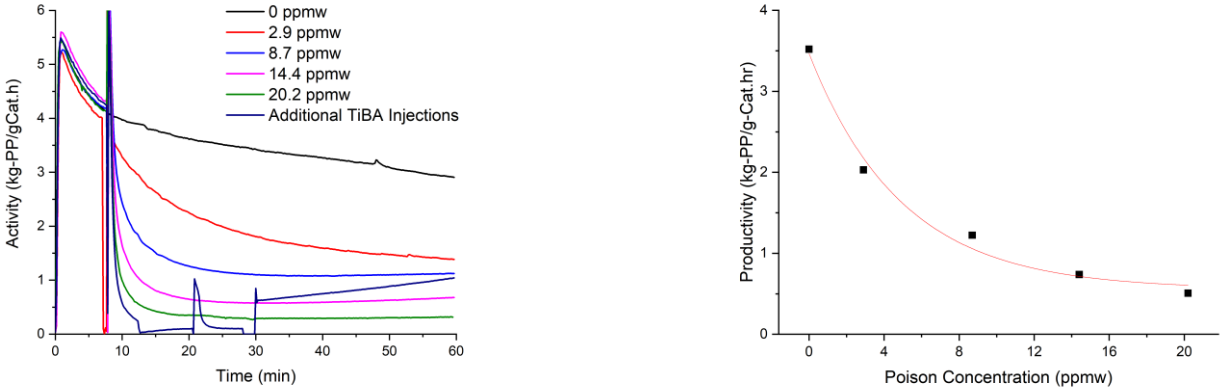


**A** **B**

***Figure 6**. **A**. Catalyst activity rates with time in propylene polymerization with $CO_2$, **B**. net catalyst activity as a function of $CO_2$ concentration.*

$O_2$ addition shows that it is the strongest among the selected poisons, a very fast and sharp drop is observed in activity followed by continuous decay in the catalyst activity as shown in **Figure 7-A**. Contrary to the $CO_2$, there is no stabilization period which makes it difficult to judge whether the poisoning reaction is reversible or not. However, the addition of TiBA twice did lead to very mild recovery in activity. The catalyst was completely deactivated when around 8 ppm of $O_2$ was added. The productivity responds linearly to the concentration of $O_2$ as shown in the fit in **Figure 7-B** with an adjusted $R^2$ of around 0.98.

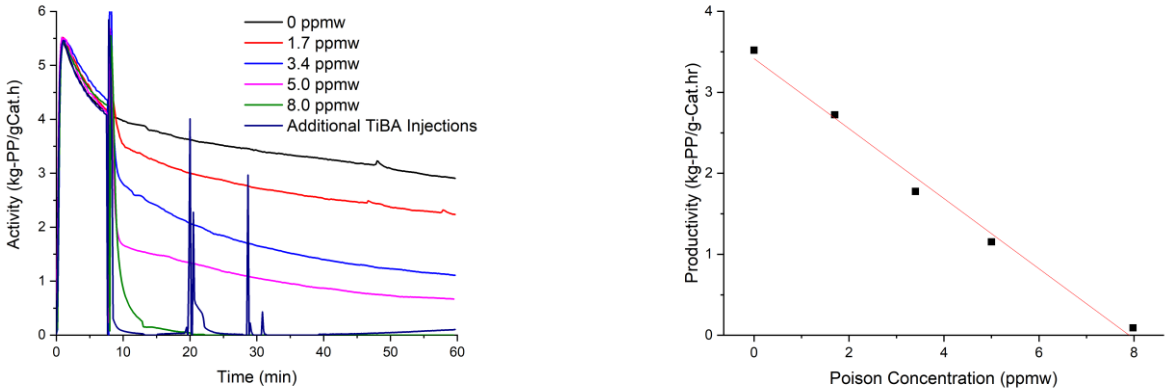


**A** **B**

***Figure 7**. **A**. Catalyst activity rates with time in propylene polymerization with $O_2$, **B**. net catalyst activity as a function of $O_2$ concentration.*

Due to the lack of a dosing system that allows for controlled additions of liquid poisons, we used the same amount of toluene (to avoid solubility effects) as a solvent for all the liquid poisons to inject the low quantities stated for each experiment. However, water is not miscible in toluene which made it tricky to add very low quantities, one of the solvents that water is miscible in is THF but THF itself is a strong catalyst poison. So, we have only performed two experiments with the lowest possible amounts of water (i.e., 1000 and 2000 ppmw). As shown in **Figure 8-A**, at those concentrations water depresses the activity quite quickly, however, even at such high concentrations the catalyst is not deactivated completely. Only in the second experiment, we can see no catalyst activity at around minute 48 of reaction. The poisoning is permanent as there were no signs of recovery after two injections of TiBA in experiment 28. Though we do not have enough data points for a robust activity response as a function of water concentration, fitting the activity using an exponential decay model follows a reasonable trend as shown in **Figure 8-B**. However, using the productivity equation based on the fit to predict the productivity for experiment 28 in which 4000 ppmw of water was added, we get a value around 0.36 (kg-PP/gCat.h) while the real activity from the experimental data was around 0.34 (kg-PP/gCat.h). The error in the model prediction for this experiment is around 6% which is quite reasonable. Finally, this catalyst system sensitivity to poisoning by water is very weak compared to $CO_2$ and $O_2$, this is a robust feature of the catalyst as water is one of the most

common impurities that are found in propylene or can ingress into the industrial production plants.

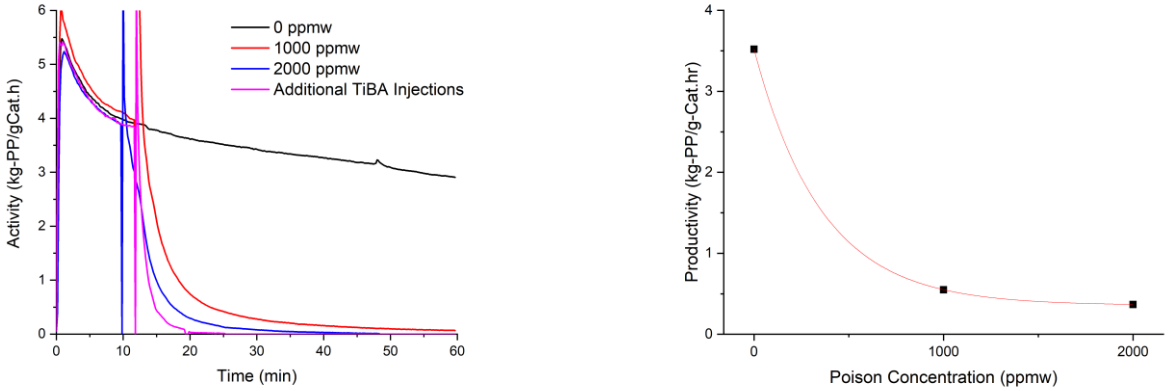


**A** **B**

***Figure 8**. **A**. Catalyst activity rates with time in propylene polymerization with $H_2O$, **B**. net catalyst activity as a function of $H_2O$ concentration.*

**Figure 9-A** shows the reaction rates after the addition of methanol at three levels: 40, 80, 633 ppmw. A fast drop in activity is observed after injecting methanol followed by a stable period for the lower concentrations, however, at the highest concentration tested, the catalyst deactivates completely almost 20 minutes after injection of methanol. Moreover, the additional injections of TiBA did not yield any observable recovery in catalyst activity. Similar to $CO_2$ and water, the activity response to methanol concentration follows an exponential decay model, as shown in **Figure 9-B** and have an $R^2$ of around 0.97.

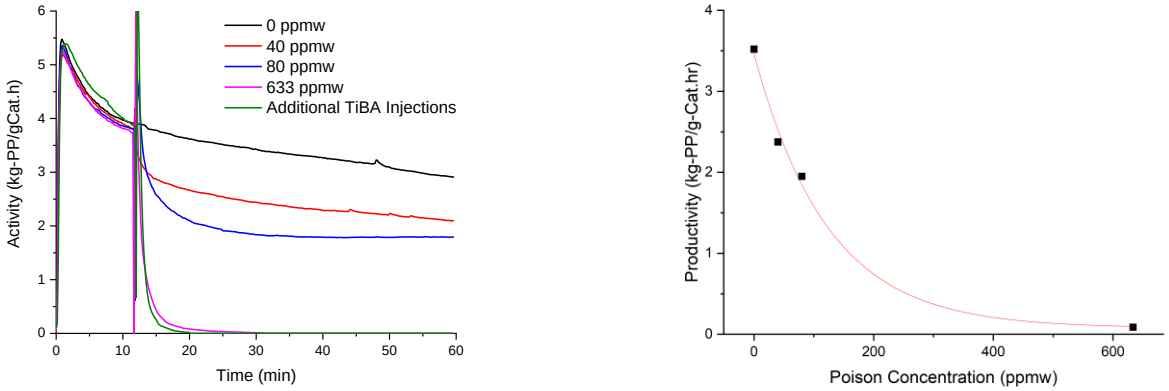


**A** **B**

***Figure 9**. **A**. Catalyst activity rates with time in propylene polymerization with methanol, **B**. net catalyst activity as a function of methanol concentration.*

The reaction rate curves with the injection of ethyl acetate are shown in **Figure 10-A**, the reaction rate is characterized by a slow exponential decay region that increases as the concentration of ethyl acetate is increased. Similar to water, and methanol; the addition of TiBA did not reverse the poisoning reaction. The response of activity to ethyl acetate concentration is shown in **Figure 10-B**, we can see that it does not show as severe a poisoning effect as the rest of the poisons.

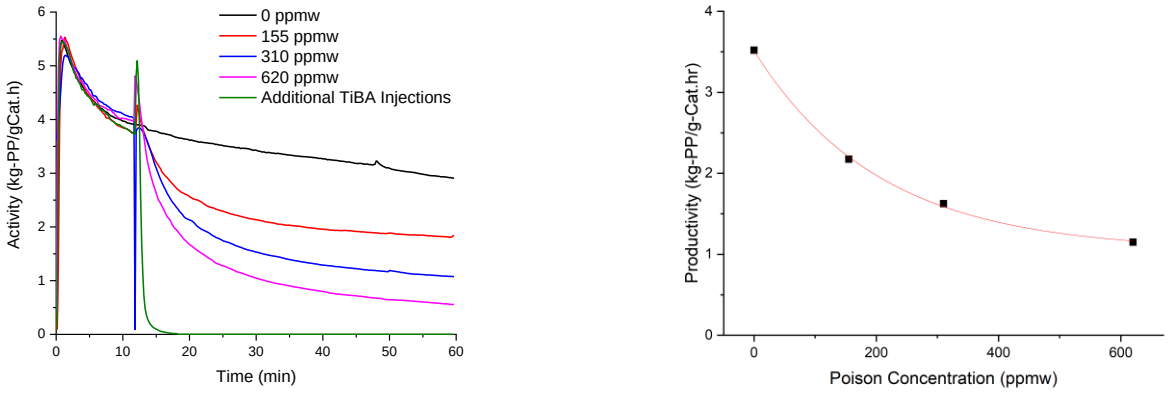


**A** **B**

***Figure 10**. **A**. Catalyst activity rates with time in propylene polymerization with ethyl acetate, **B**. net catalyst activity as a function of ethyl acetate concentration.*

DMSO is an organo-sulfur, and we have chosen it to see whether the functionality of the material changes the extent of poisoning. The reaction rates are similar to those of ethyl acetate, as shown in **Figure 11-A**, but similar amounts of DMSO lead to greater catalyst deactivation which is probably to the stronger adsorption influence by the presence of sulfur. Moreover, no signs of recovery in activity are observed after adding two shots of TiBA. **Figure 11-B** shows the productivity as a function of DMSO concentration.

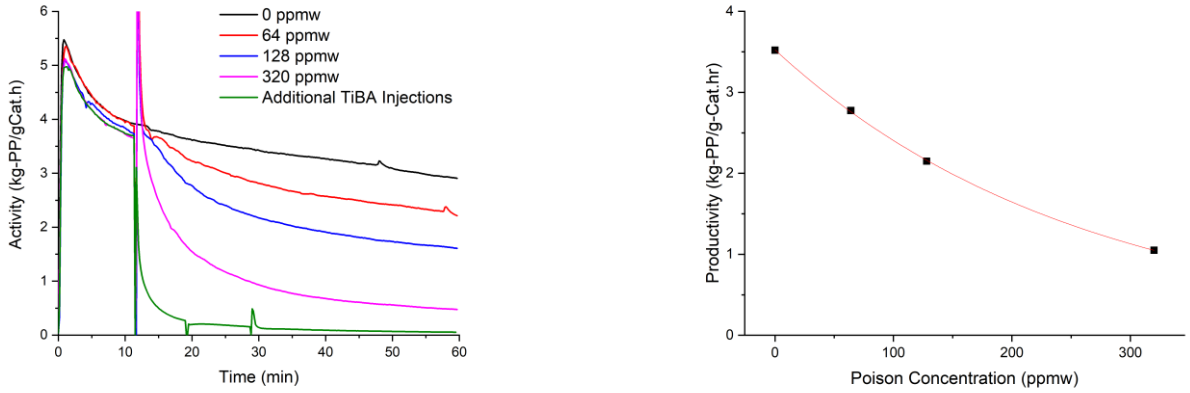


**A** **B**

***Figure 11**. **A**. Catalyst activity rates with time in propylene polymerization with dimethyl sulfoxide, **B**. net catalyst activity as a function of dimethyl sulfoxide concentration.*

When looking at all the poisons together in terms of deactivating power, we have the following trend for a 50% drop in catalyst activity: $O_2$ (3.8 ppmw) > $CO_2$ (4.4 ppmw) > $CH_3OH$ (85 ppmw) > $C_2H_6SO$ (182 ppmw) > $C_4H_8O_2$ (253 ppmw) > $H_2O$ (286 ppmw). Surprisingly, water is the least poisonous for this catalyst system which was not expected as extreme care is always taken in drying polymerization reactors in all scales to ensure the removal of moisture.

Finally, to determine the effect of these poisons on the time dependent decay, we have plotted their decay index as a function of concentration in **Figure 12**. In this case, the decay index is the rate value 5 minutes after poisons addition divided by the final rate of the reaction. $CO_2$ has almost no progressive decay effect on the reaction rate due to the reactivation of the catalyst as we have discussed earlier, $O_2$ is also similar in this aspect, as seen in **Figure 12-B**. From **Figure 12-A**, we can observe that methanol has the highest effect on decay, while water and dimethyl sulfoxide are quite similar, while ethyl acetate has the least negative impact on catalytic decay.

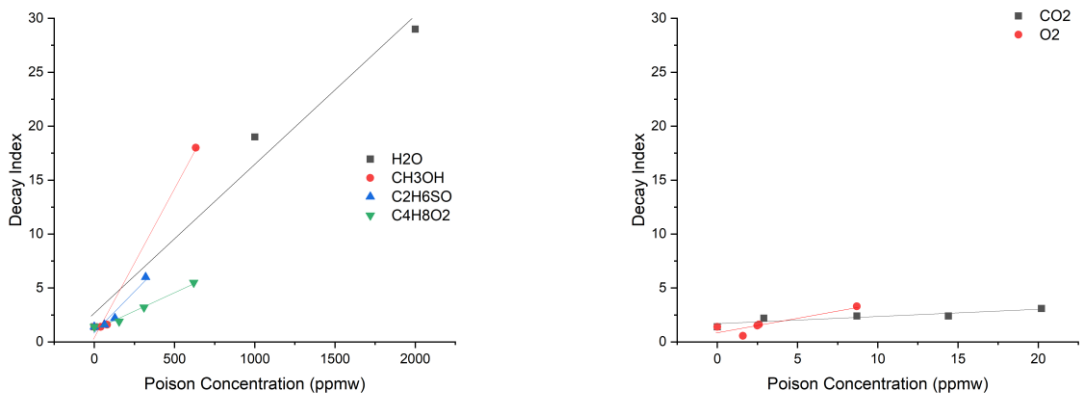


A B

***Figure 12**. Decay Indices plotted against poisons concentrations; A. $H_2O$, $CH_3OH$, $C_2H_6SO$, and $C_4H_8O_2$, B. $CO_2$ and $O_2$.*

### 3.1.3. Possible Mechanisms of Poisoning

There have not been many in-depth experimental investigations for explaining the mechanisms by which poisoning takes place in supported Ziegler Natta catalysts either with polar compounds or other electron donating compounds that are widely used since the third generation of these catalysts to control the stereoregularity in propylene polymerization. Polar compounds such as the poisons we are testing when introduced to polymerization have two possibilities of reactions; either with the co-catalyst (i.e., organoaluminums) or with the catalyst active site complex; $MgCl_2/ID/TiCl_4$. Pasynkiewicz [11] have reviewed the mechanisms of reactions of electron donating compounds with organoaluminum compounds. For the context of this work, we will look at the proposed elimination reactions with water and alcohols that proceed as follows:

$$H_2O + AlR_3 \xrightarrow{yields} HOAlR_2 + RH$$

$$ROH + AlR_3 \xrightarrow{yields} HOAlR_2 + RH$$

In both cases of water and alcohols reactions with the co-catalyst, the resulting organoaluminum product does not have the same activating power which leads eventually to a drop in activity. In practice, it is well known that whenever one suspects more impurities in the monomer feed, it is advised to ramp up the feeding of the co-catalyst to

mitigate the negative effects on catalyst productivity which is a mitigating factor in the case of occurrence of such reactions.

The reactions of oxygen with alkyl aluminums have been investigated in many references where most of these studies were conducted on the first generation catalysts. [12–14] Oxygen is believed to react with the alkyl aluminum as follows:

$$O_2 + AlR_3 \xrightarrow{yields} R_2AlOOR$$

There were conflicting effects when oxygen is reacted with the co-catalyst, activity increased for some polymerization while decreased for others. [15] More reactions with the different crystalline forms of $TiCl_3$ (first and second generation catalysts) have been proposed with varying positive and negative effects on catalyst activity depending on the form of $TiCl_3$ and the co-catalyst used. [12–15]

Reactions of alcohols and carbon oxides have been investigated extensively on the early generations of Ziegler Natta catalysts within the contexts of counting active centers. [16–19] Carbon dioxide interaction with the catalyst is believed to be a selective adsorption on the formed active centers which is reversible in nature. [16]

Although it is certain that the poisons we have used in our experiments readily react with the TiBA, however, since all the poisons have been introduced after the reaction have started, the drop in catalyst activity is most likely not completely due to reactions with the co-catalyst, their by-products, or the reduction of activating power due to the resulting organoaluminum species. It is safe to assume that most of the active sites are formed in the beginning of the reaction by the co-catalyst. Hence, the rule of the co-catalyst after the active sites are formed is not significant in relation to whether it reacts with the poisoning compounds and cause the observed decay. Thus, we believe the poisons reactions that are leading to the observed effect on the reaction rates are due to the direct adsorption and interaction with the active species complex; $MgCl_2$/ID/$TiCl_4$. A computational study published by Bahri-Laleh [20] investigating the adsorption of several poisons among which was water, $CO_2$, $O_2$ and methanol, showed that the most favorable interaction of these poisons is with the active Ti followed by Mg, and then the alkyl aluminum. Moreover, the

adsorption of these polar molecules on the $MgCl_2$ surfaces is strongest with $O_2$, then followed by $CO_2$, $H_2O$, and methanol. [20] The trend of strength of adsorption is similar to the trend of deactivating power we have reported in our experiments apart from water, which in our experiments was the least harmful to the catalyst activity. It is not clear why this catalyst system is not strongly affected by the presence of water except for the negative effects on reactor operation in terms of fouling and agglomeration. One proposition is that water is the most reactive to the alkyl aluminum which means that the extent of deactivation of the catalyst depends on the competition of this reaction and the interaction of water with the active sites complex.

Ethyl acetate, and dimethyl sulfoxide both act like conventional external electron donors (i.e., silanes) in terms of their effect on the polymer stereoregularity which will be discussed later in this work. Similar behavior has reported when aromatic ester compounds are used as electron donors and some studies have shown it to be the strongest in poisoning the active sites, and decreases the atactic portion of the polymer quite well. [21–23] Conventional silanes which are used for controlling the polymer tacticity are known to cause indiscriminate poisoning of all types of active sites beyond a specific threshold if the molecule is not bulky enough to favor selective poisoning of aspecifc sites. [24] Moreover, both ethyl acetate and dimethyl sulfoxide have been used as complexing agents with co-catalysts in polymerizations of polar monomers such as vinyl chloride, and methyl methacrylate with Ziegler Natta type catalysts and their ability to control the polymers stereoregularity whereby similar polymers as those produced using radical initiators are obtained have been observed. [25, 26]

### 3.2. Polymer Microstructure and Morphology

Polymer microstructural properties determine the application for which a specific polymer can be used. In the case of isotactic polypropylene; the molecular weight, and crystallinity which is mainly affected by isotacticity, are the determining factors for the mechanical properties of the polymer as well as processing conditions. Investigating the effects of catalyst poisons on microstructural properties have two dimensions of importance; the most crucial is the impact on the polymer quality for a specific application

industrially, and the second is to shed light on the mechanistic details of such catalysts that govern the polymer microstructure. In this study, we are focusing on the former as a part of the development work of this catalyst system. In this section, we will present the microstructural results of this experimental program. Additionally, we will look at the impact on the morphology of the polymer powder.

### 3.2.1. Molecular Weight

The effects of poisons on molecular weight characteristics have been of interest for quite a long time motivated by efforts to narrow the molecular weight distribution by selective poisoning which in theory would provide good insights on the nature of active sites. In this study, molecular weight characteristics deviations are important to anticipate discrepancies in product properties when poisons are present in the feedstock and mitigate such product quality issues. The number average molecular weight ($M_n$) is practically the same for three poisons: water, ethyl acetate, and dimethyl sulfoxide, whereas we can see a mild decrease in the cases of $CO_2$, $O_2$, and methanol at the highest concentration as seen in **Table 6**. The weight average molecular weight ($M_w$) results have a similar decreasing trend for $O_2$, $CO_2$, and Methanol while for ethyl acetate, and dimethyl sulfoxide; we can see a very mild increase at the highest concentrations. In the case of water, there is no notable change in $M_w$. There is no clear trend in the molecular weight distribution for almost all experiments, but for sure we do not observe the narrowing effect using most poisons that was seen by Arjmand et al. [7] when introducing water and carbonyl sulfide to the polymerization. On the contrary, if there is any detectable trend, it might be a mild trend of widening in MWD. The MWD curves for the highest concentration of each poison can be seen in **Figure 13**, we can see two main observations; methanol at the highest concentration yields the lowest $M_n$ with a clear shoulder at the low molecular weight end, and a broadening on the higher molecular weight side for ethyl acetate and dimethyl sulfoxide which is due to the increased transformation of aspecific sites to isospecific ones which tend to produce higher molecular weight chains.

***Table 6**. Molecular weight characteristics.*

| SN | Poison | Poison Concentration (ppmw) | Mn (kDa) | Mw (kDa) | MWD | MzR |
|---|---|---|---|---|---|---|
| 10 | None | 0.0 | 30 | 182 | 6.1 | 4.2 |
| 12 | $CO_2$ | 2.9 | 26 | 175 | 6.8 | 3.9 |
| 13 | $CO_2$ | 8.7 | 22 | 170 | 7.7 | 2.3 |
| 14 | $CO_2$ | 14.4 | 25 | 169 | 6.8 | 3.0 |
| 15 | $CO_2$ | 20.2 | 27 | 165 | 6.2 | 2.9 |
| 17 | $O_2$ | 1.7 | 29 | 182 | 6.2 | 3.0 |
| 18 | $O_2$ | 3.4 | 23 | 170 | 7.3 | 2.8 |
| 19 | $O_2$ | 5.0 | 26 | 165 | 6.4 | 2.3 |
| 20 | $O_2$ | 8.0 | 26 | 161 | 6.2 | 3.8 |
| 22 | $H_2O$ | 1000.0 | 30 | 179 | 6.1 | 2.2 |
| 23 | $H_2O$ | 2000.0 | 28 | 174 | 6.1 | 2.8 |
| 25 | $CH_3OH$ | 40.0 | 26 | 172 | 6.5 | 3.5 |
| 26 | $CH_3OH$ | 80.0 | 28 | 158 | 5.6 | 2.0 |
| 27 | $CH_3OH$ | 633.0 | 17 | 154 | 8.9 | 2.6 |
| 29 | $C_4H_8O_2$ | 155.0 | 34 | 178 | 5.3 | 3.3 |
| 30 | $C_4H_8O_2$ | 310.0 | 33 | 179 | 5.4 | 1.9 |
| 31 | $C_4H_8O_2$ | 620.0 | 25 | 196 | 7.8 | 2.5 |
| 33 | $C_2H_6SO$ | 64.0 | 30 | 170 | 5.7 | 2.2 |
| 34 | $C_2H_6SO$ | 128.0 | 28 | 168 | 6.0 | 1.9 |
| 35 | $C_2H_6SO$ | 320.0 | 29 | 195 | 6.7 | 3.6 |

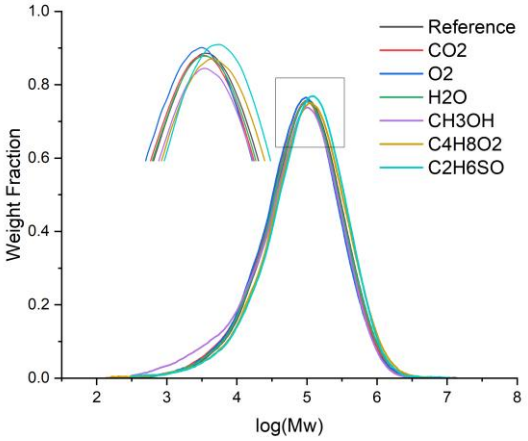


***Figure 13**. Molecular weight distributions for the reference, and the highest poison concentration experiments.*

Another characteristic parameter in molecular weight that is not frequently reported is the higher molecular weight averages ratio (MzR); $M_{z+1}$ divided by $M_z$ which basically represents the high molecular weight portion of the polymer. Controlling higher

molecular weight tails is quite an important parameter for effective polymer processing. For example, for spun bond fibers polymer grades, it is preferable to have a lower MzR in order to avoid breaking of fiber and allow the polymer to disentangle quickly during fiber spinning. [27] Comparing the poisons experiments to the reference, we can observe an overall decrease in this ratio. This is most likely due to the tendency of poisoning higher molecular weight producing sites which results in the observed drop in the high molecular weight tails.

### 3.2.2. Crystallinity

Melting ($T_m$) and crystallization ($T_c$) temperatures are presented in **Table 7** where we can clearly see that there are no differences as a function of the amount and type of poison. This is expected as these poisons do not affect the chain morphology but rather affect the chemical nature of active sites. However, crystallinity fractions ($X_c$) presented in the same table shows some changes, a decreasing trend can be observed for $CO_2$, $O_2$, $H_2O$, and Methanol. This is due to the drop of stereoregular control that is most likely because of the preferential poisoning of highly isotactic sites which is also seen in the increase of soluble fraction of the polymer which will discussed in the upcoming section. On the other hand, a mild increase in crystallinity is observed with ethyl acetate and dimethyl sulfoxide which is corresponding to a decrease in the atactic portion of the polymer.

One interesting characteristic of crystallization we are showing in **Figure 14** is the width of the crystallization peak for all the experiments which is an indication of the size distribution of crystallites. For all the poisons expect dimethyl sulfoxide, there is a clear narrowing of the peak by at least 1 °C, whereas a mild increase by up to 1 °C is observed for dimethyl sulfoxide. The distribution of crystallites can be affected by several parameters among which are the length of the polymer chains, and the tacticity of the polymer. [28–30] The drop in iso-tacticity and mild decrease in molecular weight explain this narrowing effect except for ethyl acetate for which we are not sure what is causing the narrowing effect though the molecular weight is following a similar pattern as with the dimethyl sulfoxide for which the crystallites size distribution is broader.

***Table 7**. Melting, crystallization temperatures, and crystallinity fraction.*

| SN | Poison | Poison Concentration (ppmw) | $T_m$ (°C) | $T_c$ (°C) | $X_c$ (%) |
|---|---|---|---|---|---|
| 10 | None | 0.0 | 160 | 120 | 48 |
| 12 | $CO_2$ | 2.9 | 160 | 121 | 47 |
| 13 | $CO_2$ | 8.7 | 160 | 122 | 45 |
| 14 | $CO_2$ | 14.4 | 160 | 122 | 44 |
| 15 | $CO_2$ | 20.2 | 160 | 121 | 44 |
| 17 | $O_2$ | 1.7 | 160 | 121 | 44 |
| 18 | $O_2$ | 3.4 | 160 | 122 | 43 |
| 19 | $O_2$ | 5.0 | 160 | 123 | 42 |
| 20 | $O_2$ | 8.0 | 160 | 121 | 42 |
| 22 | $H_2O$ | 1000.0 | 161 | 123 | 46 |
| 23 | $H_2O$ | 2000.0 | 160 | 121 | 45 |
| 25 | $CH_3OH$ | 40.0 | 160 | 121 | 47 |
| 26 | $CH_3OH$ | 80.0 | 160 | 121 | 45 |
| 27 | $CH_3OH$ | 633.0 | 161 | 121 | 44 |
| 29 | $C_4H_8O_2$ | 155.0 | 162 | 122 | 51 |
| 30 | $C_4H_8O_2$ | 310.0 | 162 | 122 | 51 |
| 31 | $C_4H_8O_2$ | 620.0 | 162 | 122 | 53 |
| 33 | $C_2H_6SO$ | 64.0 | 161 | 121 | 52 |
| 34 | $C_2H_6SO$ | 128.0 | 161 | 122 | 54 |
| 35 | $C_2H_6SO$ | 320.0 | 162 | 121 | 56 |

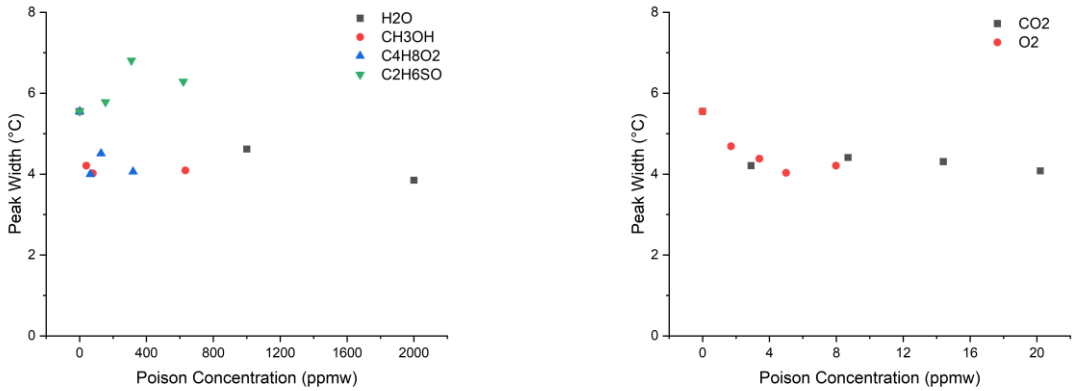


**A** **B**

***Figure 14**. Crystallinity peaks widths for: **A**. $H_2O$, $CH_3OH$, $C_2H_6SO$, and $C_4H_8O_2$, **B**. $CO_2$ and $O_2$.*

### 3.2.3. Tacticity

Tacticity is the measurement of polypropylene stereoregularity that is mostly inferred industrially using a standard test called "xylene solubles (XS)". This test quantifies

the soluble portion of the polymer in a solvent, in this case; xylene, which are mostly atactic polymer and oligomers. More advanced techniques have been utilized historically for tacticity quantification; most widely $^{13}C$ NMR. More recently, techniques like Crystallization Elution Fractionation (CEF) have been utilized to distinguish isotactic and atactic portions of the polymer. Busico et al. [31] have shown that there is a very good correlation between XS, and the soluble fraction (SF) detected by CEF.

The SF results for our experiments in this study computed from CEF analysis are shown in **Table 8**. $CO_2$ and $O_2$ both have a similar effect where we can see a similar increase in the SF which means there is less stereoregular control when these poisons are introduced. This effect is due to the poisoning of highly isotactic sites, this same effect is observed as seen earlier in the effect on polymer crystallinity, a good trend between SF and crystallinity is observed as shown in **Figure 16**. In the case of water, we see an increase in SF but given the fact that its concentration was quite high, it is not as effectively affecting stereoregularity as $CO_2$ and $O_2$. Methanol severely affects the stereoregularity, but as in the case of water, the concentrations of methanol were much higher than those of $CO_2$, and $O_2$. This simply shows that the trend of shifting XS or SF correlates with the power of deactivation of the poison. In practical terms, if such a poison is causing only a mild drop in activity, not much drift in isotacticity is expected. If we plot activity against the SF for $CO_2$, $O_2$, Methanol, and water experiments, we can observe a clear decreasing trend of soluble fraction as activity increases, shown in **Figure 15**. This trend reverses in the cases of ethyl acetate and dimethyl sulfoxide indicating the ability of these two poisons to regulate tacticity acting in a comparable way to conventional external electron donors: silanes for example.

CEF profiles for all experiments are shown in **Figure 17**, there are two main peaks, the magnified portion is the polymer that elutes at room temperature which is mostly atactic polymer, and oligomers, while the second is the isotactic part that elutes at a similar temperature for all experiments, around 118 °C. A mild shift is seen in the elution of the isotactic part for ethyl acetate and dimethyl sulfoxide can be observed due to the increase in isotacticity of these polymer.

***Table 8**. Soluble fraction results obtained from CEF with the different poisons.*

| SN | Poison | Poison Concentration (ppmw) | Soluble Fraction (wt%) |
|---|---|---|---|
| 10 | None | 0.0 | 8.13 |
| 12 | $CO_2$ | 2.9 | 8.96 |
| 13 | $CO_2$ | 8.7 | 9.05 |
| 14 | $CO_2$ | 14.4 | 9.25 |
| 15 | $CO_2$ | 20.2 | 11.2 |
| 17 | $O_2$ | 1.7 | 8.83 |
| 18 | $O_2$ | 3.4 | 10.8 |
| 19 | $O_2$ | 5.0 | 11.1 |
| 20 | $O_2$ | 8.0 | 11.7 |
| 22 | $H_2O$ | 1000.0 | 10.3 |
| 23 | $H_2O$ | 2000.0 | 10.6 |
| 25 | $CH_3OH$ | 40.0 | 8.37 |
| 26 | $CH_3OH$ | 80.0 | 9.11 |
| 27 | $CH_3OH$ | 633.0 | 11.7 |
| 29 | $C_4H_8O_2$ | 155.0 | 5.91 |
| 30 | $C_4H_8O_2$ | 310.0 | 5.38 |
| 31 | $C_4H_8O_2$ | 620.0 | 5.25 |
| 33 | $C_2H_6SO$ | 64.0 | 6.44 |
| 34 | $C_2H_6SO$ | 128.0 | 5.87 |
| 35 | $C_2H_6SO$ | 320.0 | 4.99 |

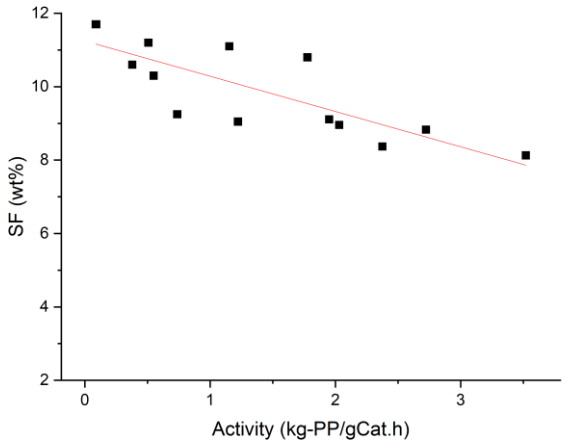


***Figure 15**. Soluble fraction plotted against activity for $CO_2$, $O_2$, Methanol, and water.*

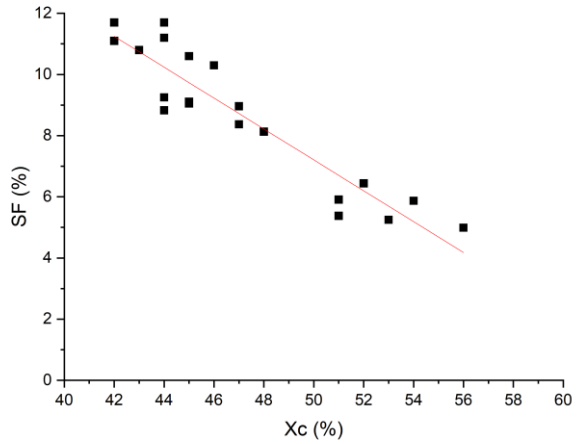


***Figure 16**. Correlation between the SF and Xc for all poisons experiments.*

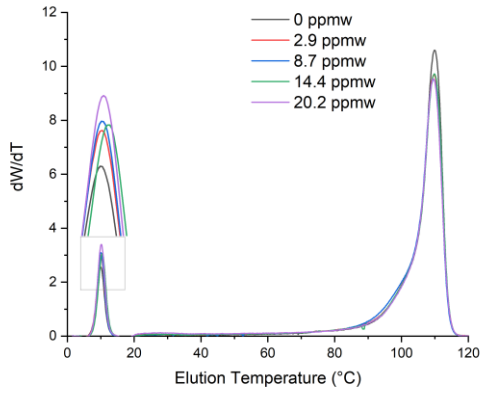


**A**

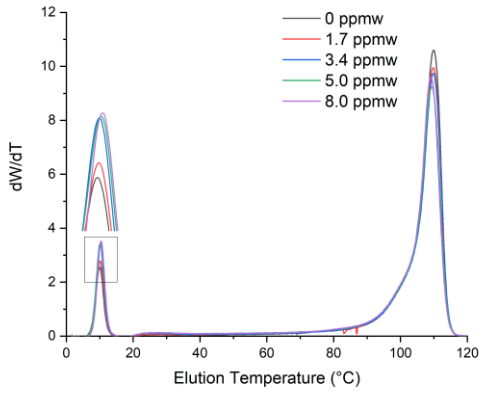


**B**

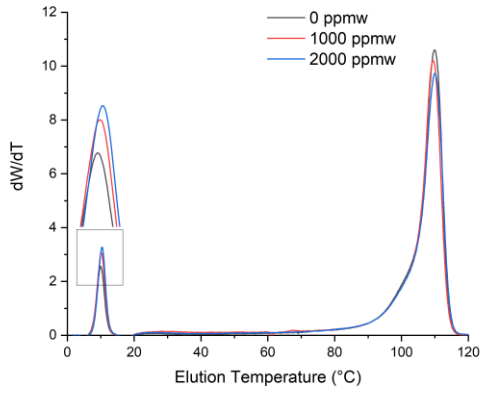


**C**

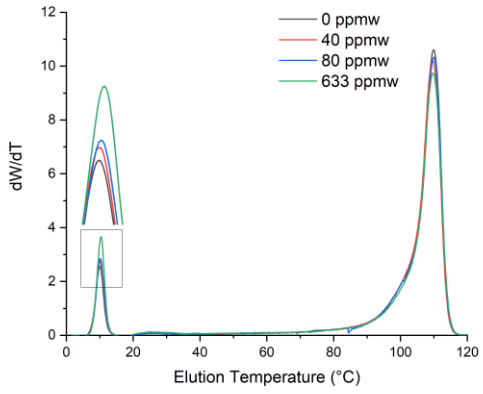


**D**

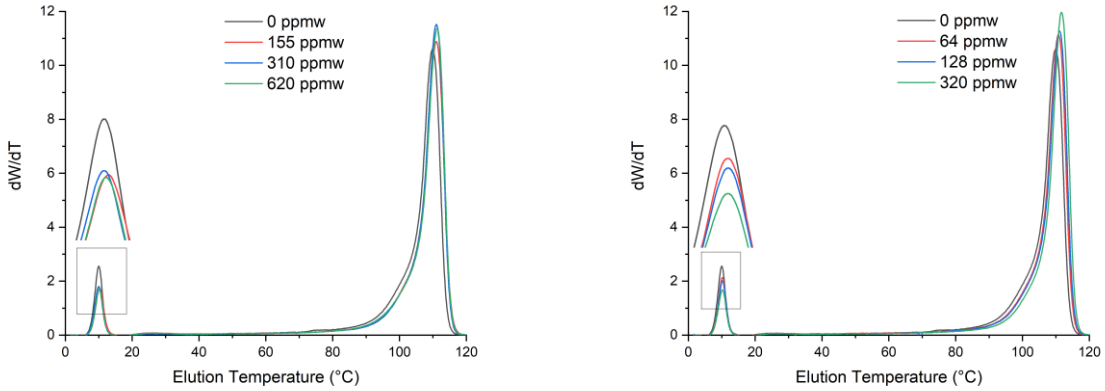


**E** **F**

***Figure 17****. CEF profiles for:* ***A****.* $CO_2$*,* ***B****.* $O_2$*,* ***C****.* $H_2O$*,* ***D****.* $CH_3OH$*,* ***E****.* $C_4H_8O_2$*, and* ***F****.* $C_2H_6SO$*.*

### 3.2.4. Resin Morphology

Resin (powder) morphology is quite important for gas phase processes and is usually characterized industrially using two main tests: loose bulk density, and fines content. Bulk density for polymer powder is a parameter that is critical for the design phase of the process, and operation; usually decreasing bulk densities are not desired even slightly. Fines are a measurement of the percentage of powders below a specific size, industrially taken to be 120 μm, which is always desired to be at the minimum as more fine particles lead to higher fouling rates which results in more frequency of cleaning and maintenance of the process at the least.

**Figure 18** shows the bulk density of the produced polypropylene as a function of poison concentration. There is a very mild increase in bulk density for the lower concentrations of $CO_2$ and $O_2$, but it isn't sustained at higher concentration, the bulk density starts to decrease slightly for $CO_2$ and more significantly for $O_2$ at higher concentrations. The highest decrease in bulk density is observed with water, the rest of the liquid poisons have no effect or a mild positive effect in the case of ethyl acetate.

The particle size average and cumulative distributions for the reference experiments and the highest concentrations with the poisons are presented in **Figure 19** where we can see in both graphs a clear shift in the distribution to the lower size with $CO_2$

and $O_2$, whereas for water and methanol, the distribution spans a similar range as the reference experiments. This shifting to the lower size is due to the deactivation of active sites which then limits particle growth. A similar broadening is observed as well with ethyl acetate and dimethyl sulfoxide but with a milder increase in the higher particle size end. One important parameter that is taken from this analysis is the fines content (less than 45 µm for this scale), the results are shown in **Figure 20**. The highest levels of fines generation are seen with $CO_2$, $O_2$, and water reaching around 3 wt% while the rest of the poisons reach around 2% at the highest concentrations. A clear trend is observed between the fines content and activity drop for $CO_2$, $O_2$, Methanol, and water which can be of practical utility for the higher production scales, shown in **Figure 21** which is expected as poisons' deactivation of the catalyst leads to inhibition in the growth of polymer particles.

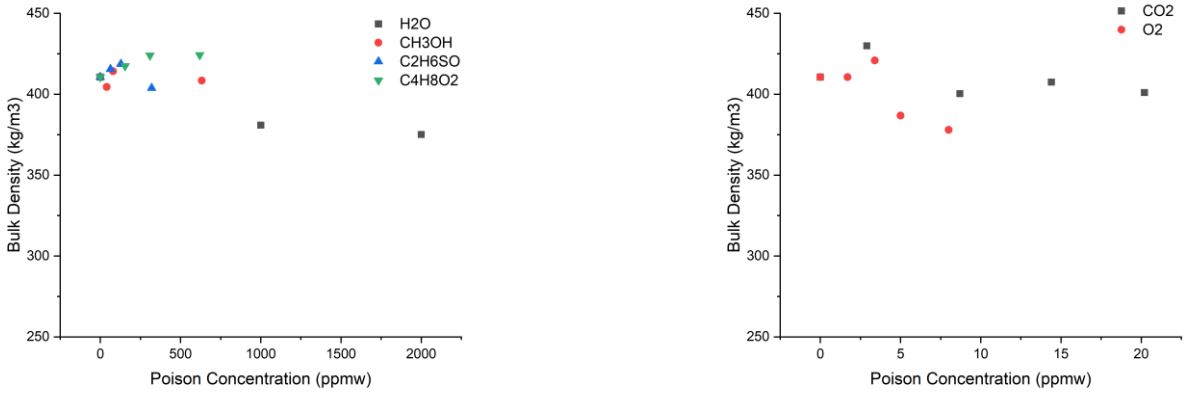


**A** **B**

***Figure 18****. Resin bulk density changes as a function of poisons concentration; A. $H_2O$, methanol, dimethyl sulfoxide, and ethyl acetate, and B. $CO_2$, and $O_2$.*

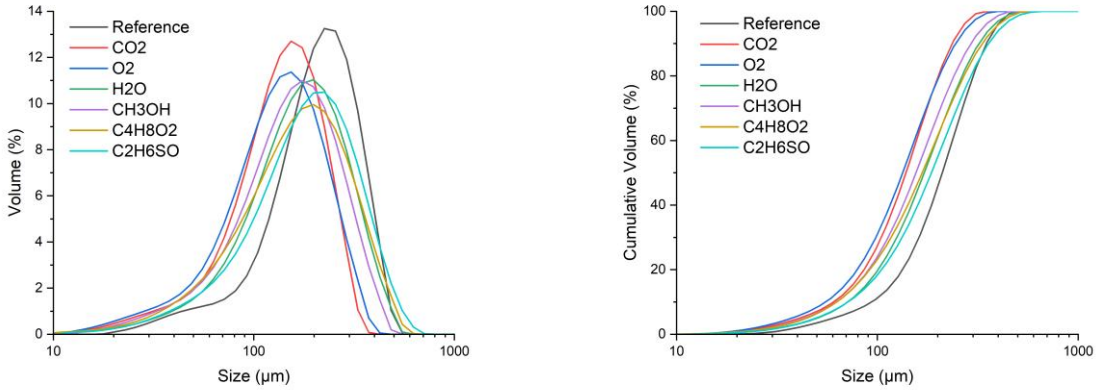


A B

***Figure 19**. PSD for the reference and poisons at the highest concentration; A. average, and B. cumulative.*

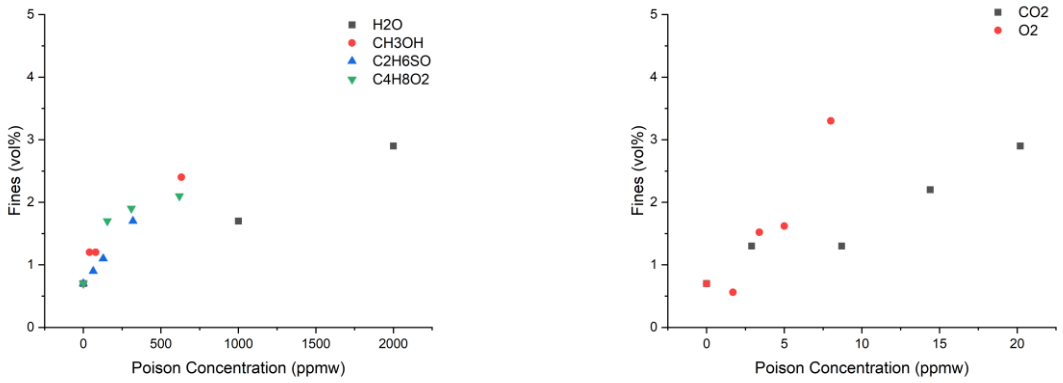


A B

***Figure 20**. Fines content plotted against poison concentration; A. $H_2O$, methanol, dimethyl sulfoxide, and ethyl acetate, and B. $CO_2$, and $O_2$.*

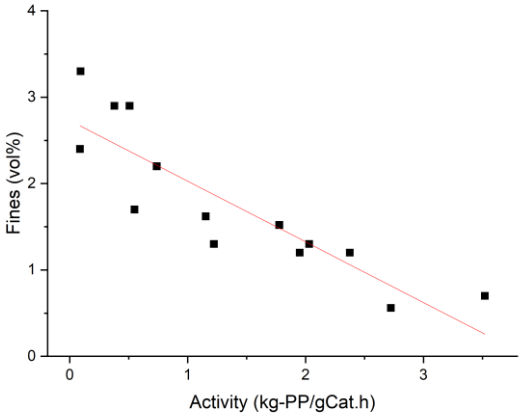


***Figure 21**. Fines content plotted against activity.*

### 3.3. Reactor Fouling and Resin Agglomeration

Fouling is a serious yet a frequent problem in gas phase fluidized bed polymerization reactors. The consequences of fouling can range from difficulties in operating the reactor to completely shutting down the plant but certainly comes at a cost in all of its forms. Fouling in said reactors can be categorized to three different types: powder film depositing on the walls and inside the internal parts of the different operation units in the reaction area, polymer sheets formation on the walls of the reactor, and formation of agglomerates that can be of any size with the worst scenario being that most or all the bed

agglomerates to form one huge lump. There are mainly three underlying phenomenon that facilitates fouling: the generation of fine particles in the fluidizing bed, the accumulation in the bed's static electricity charge, and the adhesion of particles together.

**Figure 22** shows pictures of the reactor body and agitator; A. after the reference reaction, where one can observe much less deposition of particles on both the wall and the agitator, B. the reaction with water added as a poison, and C. the reaction with methanol. For both cases of water and methanol, it can be seen clearly that there is a lot of deposition of particles on the wall and agitator. This has been observed only with water and methanol, probably due to the higher polarity of these compounds affecting the overall electrostatic charge in the bed and causing stronger interactions between the particles and the surfaces of the reactor. [32] The relative polarities of methanol, dimethyl sulfoxide, and ethyl acetate to water are shown in **Table 9**. Additionally, there could be a cooperative effect between the electrostatic charge of the bed and the elevated fines content. Though the implications are nonexistent for this reactor besides spending more time on cleaning, in the pilot and commercial scales, coating the reactor walls leads to instabilities in controlling the reactor and deviations in process parameters detection instruments and eventually might lead to the formation of sheets. [33]

***Table 9**. Relative polarities for the liquid poisons.* [34]

| Compound | Relative polarity |
|---|---|
| Water | 1.0 |
| Methanol | 0.8 |
| Dimethyl Sulfoxide | 0.4 |
| Ethyl Acetate | 0.2 |

The other destabilizing phenomena we have observed with some of the poisons experiments is the formation of agglomerates. It is quite normal to have some form of agglomerates at all times in a polymerization fluidized bed reactor due to combination of factors; localized temperature excursions, particles colliding and adhering to each other, electrostatic charges, and so on. The weight percentage of agglomerates (i.e., particles larger than 4 mm) of the total yield of each reaction is plotted as a function of poison

concentration in **Figure 23**. We can see that there are agglomerates in the reference reaction, however, it is much less than 1 wt% of the total polymer weight, whereas with water and methanol, we see a significant increase in agglomeration by a factor of around 5 to 8. On the other hand, with the other tested poisons, such behavior is not observed, in fact, there is a slight decrease in formation of agglomerates noticeably with ethyl acetate, and dimethyl sulfoxide which is probably due to the decrease in the soluble fractions in those experiments which results in less sticky powders. In the case of oxygen and carbon dioxide, there is no notable change, but a very mild decrease can be observed. This is most likely due to the effectiveness of these two poisons in rendering the catalyst active sites completely dead which decreases the probability of forming localized hot zones that eventually leads to particles adhering to each other. However, this is certainly not the only factor at play here, if we look at ethyl acetate and dimethyl sulfoxide, we can see a clear decrease, knowing that a clear distinguishing factor between the two cases is the content of soluble fraction of the polymer gives a hint that stickiness of the powder is an important facilitating parameter for adhesion. However, the soluble fraction is quite similar for oxygen, and carbon dioxide to that of water and methanol, yet we do not see much agglomeration happening. This behavior can be explained by the polarity of these two components leading to accumulation and disturbances in the electrostatic charge inside the reactor which in turns facilitates particles adhering to each other especially the fine particles. So, we can define three different parameters which are in this case important in determining formation of agglomerates; stickiness of the polymer (i.e. soluble fraction), static electricity changes due to polarity of poisons [32] , and localized hot spots within the polymerizing bed. Photographic examples of such agglomerates are shown in **Figure 24**.



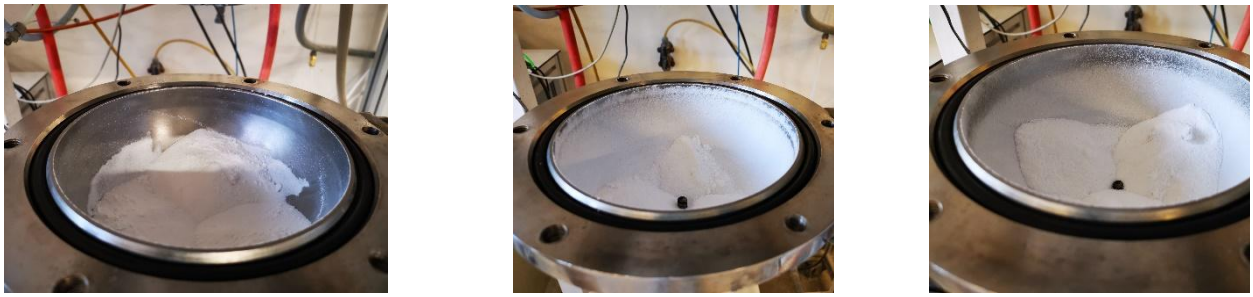

**A** **B** **C**

***Figure 22****. Photos of the reactor internals post experiment; A. a standard reaction, B. with $H_2O$, and C. with Methanol.*

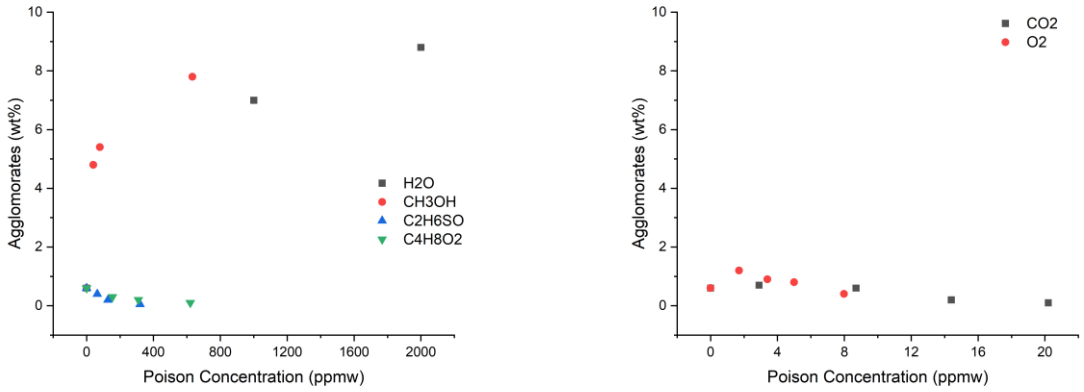


**A** **B**

***Figure 23****. Agglomerates content in propylene polymerization experiments;* ***A****. $H_2O$, methanol, dimethyl sulfoxide, and ethyl acetate, and* ***B****. $CO_2$, and $O_2$.*

***Figure 24****. photos of some of the agglomerates recovered from the reactions with the poisons.*

## 4. Conclusions

In this work, we have studied the effects of catalyst poisons on reaction kinetics, microstructural properties, and powder morphology in gas phase propylene

polymerization using 6th generation Ziegler Natta catalysts. We have used two approaches to achieve this, firstly, we have used propylene without purification, with one set, and two sets of purification columns, the second approach was introducing carbon dioxide ($CO_2$), and oxygen ($O_2$), water ($H_2O$), methanol ($CH_3OH$), ethyl acetate ($C_4H_8O_2$), and dimethyl sulfoxide ($C_2H_6SO$) during the polymerization reaction.

In the first part, we have observed the significant effect of on catalyst activity when passing propylene through one set of purification columns, and increase of more than 200%, additional set of columns have resulted in a further 30% increase in catalyst activity. Moreover, a mild decrease in catalyst decay was observed with the addition of purification columns that becomes more pronounced at higher reaction temperatures. The effect of purification columns on activity is sustained with two different co-catalysts, TEA, and TiBA for which the activity is higher in all conditions (i.e., without and with purification) which is probably due to a higher scavenging power of TiBA. Additionally, injecting TiBA during the polymerization in the absence of purification columns for the monomer results in a noticeable increase in activity. Nevertheless, one of the interesting observations that we have noticed with these experiments was the significant repeatability of reactions when two sets of purification columns in contrast to one set of columns.

The addition of select poisons during the reaction at different concentrations showed how the reaction rate is affected and eventually the productivity of the catalyst. The strength of poisoning was as follows: $O_2$ > $CO_2$ > $CH_3OH$ > $C_2H_6SO$ > $C_4H_8O_2$ > $H_2O$, where the poisoning of active sites most likely proceeds by direct adsorption, and by reducing the activating power of the co-catalyst. The deactivation caused by the poisons was only reversible for $CO_2$, and mildly for $O_2$, as observed after additional injections of the co-catalysts are administered. All poisons resulted in an increase in the decay index with water and methanol exhibiting the strongest influence, whereas CO2 and O2 only mildly increase the decay which is due to the competition between the poison adsorption reactions, and the reactivation reactions.

We have also investigated the effect of the injected poisons on the polymer microstructural properties, and powder morphology. The addition of $CO_2$, $O_2$, and $CH_3OH$

resulted in a progressive decrease in molecular weight, while no significant effect was observed with $H_2O$. On the other hand, $C_4H_8O_2$, and $C_2H_6SO$ resulted in a mild increase in molecular weight at the higher concentrations which is due to their stereo-regulating effect that is evident from the soluble fraction analysis. The soluble fraction of the polymer which is a measure of isotacticity of the polymer was increasing with all poisons, meaning that the poisons are reducing the isotacticity of the polymer, except with $C_4H_8O_2$, and $C_2H_6SO$ where the soluble fraction reduced. The same behavior is also reflected in polymer crystallinity where it progressively decreased except for $C_4H_8O_2$, and $C_2H_6SO$. Powder morphology was affected negatively with some poisons as measured by two characteristics: fines content, and agglomerates weight percentage. Fines content increased with all poisons which is expected as the overall particle size of the polymers decreases significancy due to the retarding effect on catalyst activity which leads to diminished growth of particles. The weight of agglomerates, particles larger than 4 mm, was only observed with water and methanol which is due to a combination of factors, but mainly, the high polarity of these compounds influences the electrostatic charges in the bed which could lead to more particles drawn to the reactor wall and each other.

## References


1. Pernusch DC, Spiegel G, Paulik C, Hofer W (2022) Influence of Poisons Originating from Chemically Recycled Plastic Waste on the Performance of Ziegler–Natta Catalysts. Macromol React Eng 16:1–10. https://doi.org/10.1002/mren.202100020

2. Pernusch DC, Paulik C, Mastalir M, Hofer W (2022) Assessing the Downstream Contamination of Chemically Recycled Ethylene Feed Streams on the Kinetic Behavior of Ziegler-Natta Catalysts and Microstructural Properties of HDPE and LLDPE. Macromol React Eng 2200042:2200042. https://doi.org/10.1002/mren.202200042

3. Pernusch DC, Spiegel G, Paulik C, Hofer W (2022) Nitrogen Poisoning of HDPE and LLDPE based on Chemically Recycled Post-Consumer Plastic via a Kinetic and Microstructural Modeling Technique. Macromol React Eng 2200006:1–13. https://doi.org/10.1002/mren.202200006

4. Choi KY, Ray WH (1985) Polymerization of olefins through heterogeneous catalysis. I. Kinetics of gas phase propylene polymerization with Ziegler–Natta catalysts. J Appl Polym Sci 30:1065–1081. https://doi.org/10.1002/app.1985.070300315

5. Vizen EI, Rishina LA, Sosnovskaja LN, et al (1994) Study of hydrogen effect in propylene polymerization on (with) the MgCl2-supported ziegler-natta catalyst-part 2. Effect of CS2 on polymerization centres. Eur Polym J 30:1315–1318.

https://doi.org/10.1016/0014-3057(94)90144-9

6. Tangjituabun K, Yull Kim S, Hiraoka Y, et al (2008) Effects of various poisoning compounds on the activity and stereospecificity of heterogeneous Ziegler-Natta catalyst. Sci Technol Adv Mater 9:. https://doi.org/10.1088/1468-6996/9/2/024402

7. Arjmand S, Shakeri A, Arabi H (2019) Effect of water and carbonyl sulfide toxins in gas propylene feed in polymerization process on physical properties of polypropylene. J Polym Res 26:. https://doi.org/10.1007/s10965-019-1860-z

8. Bershtein VA., Egorov VM, Leib G V, et al (1994) Differential Scanning Calorimetry of Polymers: Physics, Chemistry, Analysis, Technology. Ellis Horwood, New York

9. Keii T, Suzuki E, Tamura M, et al (1982) Propene polymerization with a magnesium chloride-supported ziegler catalyst, 1. Principal kinetics. Die Makromol Chemie 183:2285–2304. https://doi.org/10.1002/macp.1982.021831001

10. Han-Adebekun GC, Ray WH (1997) Polymerization of olefins through heterogeneous catalysis. XVII. Experimental study and model interpretation of some aspects of olefin polymerization over a TiCl4/MgCl2 catalyst. J Appl Polym Sci 65:1037–1052. https://doi.org/10.1002/(SICI)1097-4628(19970808)65:6<1037::AID-APP1>3.0.CO;2-L

11. Pasynkiewicz S (1972) Reactions of organoaluminium compounds with electron donors. Pure Appl Chem 30:509–522. https://doi.org/10.1351/pac197230030509

12. Schnecko H, Lintz W, Kern W (1967) Polymerization with heterogeneous metalorganic catalysts. VI. Differences in polymerization activity of α-olefins and some kinetic results on butene-1 polymerization. J Polym Sci Part A-1 Polym Chem 5:205–214. https://doi.org/10.1002/pol.1967.150050119

13. Martin VH, Blanck E (1963) Über Den Einfluß Von Sauerstoff Auf Titanhaltige Metallorganische Mischkatalysatoren. Die Makromol Chemie 69:1–17. https://doi.org/10.1002/macp.1963.020690101

14. Masuda T, Takami Y (1977) Effect of oxygen on Et2AlCl-TiCl3 catalyst for propylene polymerization. J Polym Sci Polym Chem Ed 15:2033–2036. https://doi.org/10.1002/pol.1977.170150824

15. Kissin Y V. (1985) Isospecific Polymerization of Olefins. Springer New York, New York, NY

16. Lesná M, Mejzlík J (1978) Influence of carbon dioxide and carbon monoxide on the kinetics of propylene polymerization. React Kinet Catal Lett 9:99–103. https://doi.org/10.1007/BF02070376

17. Mejzlík J, Lesná M (1977) Determination of active centers in heterogeneous Ziegler-Natta catalytic systems using carbon oxides. Die Makromol Chemie 178:261–266. https://doi.org/10.1002/macp.1977.021780127

18. Warzelhan V, Burger TF, Stein DJ (1982) Über die bestimmung der zahl polymerisationsaktiver zentren von ziegler-natta-katalysatoren. Eine modifizierte methode mit 14C-markierten kohlenstoffoxiden. Die Makromol Chemie 183:489–504. https://doi.org/10.1002/macp.1982.021830218

19. Mejzlík J (1986) Determination of the number of active centers in Ziegler-Natta polymerizations of olefins. Makromol Chemie Macromol Symp 3:359–376. https://doi.org/10.1002/masy.19860030127

20. Bahri-Laleh N (2016) Interaction of different poisons with MgCl 2 /TiCl 4 based Ziegler-Natta catalysts. Appl Surf Sci 379:395–401. https://doi.org/10.1016/j.apsusc.2016.04.034

21. Guyot A, Bobichon C, Spitz R, et al (1988) Transition Metals and Organometallics as Catalysts for Olefin Polymerization. Springer Berlin Heidelberg

22. Kissin Y V, Sivak AJ (1984) MODIFICATION MECHANISM IN OLEFIN POLYMERIZATION CATALYSTS TiCl4/MgCl2-AROMATIC ESTER-Al(C2H5)3. J Polym Sci A1 22:3747–3758. https://doi.org/10.1002/pol.1984.170221212

23. Maiyer EA, Bukatov GD, Rasskazov AN, Zakharov VA (1991) Polymerization of

propylene on highly active titanium-magnesium catalysts in a liquid monomeric medium. Polym Sci USSR 33:2353–2359. https://doi.org/10.1016/0032-3950(91)90286-Y

24. Sacchi M, Forlini F, Tritto I, et al (1992) Activation Effect of Alkoxysilanes as External Donors in MgCl2-Supported Ziegler-Natta Catalysts. Macromolecules 25:5914–5918. https://doi.org/10.1021/ma00048a009

25. Akimoto A (1972) Polymerization of methyl methacrylate with AlEt3–VOCl3–dimethyl sulfoxide system. J Polym Sci Part A-1 Polym Chem 10:3113–3118. https://doi.org/10.1002/pol.1972.170101029

26. Akimoto A, Yoshida T (1972) Polymerization of vinyl chloride and copolymerization with propylene by a ternary catalyst system. J Polym Sci Part A-1 Polym Chem 10:993–1000. https://doi.org/10.1002/pol.1972.150100404

27. Kaarto JK, Egmond JW Van, Lester CD (2018) PROPYLENE - BASED POLYMER WITH REDUCED HIGH - MOLECULAR WEIGHT PORTION

28. Guan Y, Wang S, Zheng A, Xiao H (2003) Crystallization behaviors of polypropylene and functional polypropylene. J Appl Polym Sci 88:872–877. https://doi.org/10.1002/app.11668

29. Yu H, Kang J, Chen J, Xiang M (2016) Effects of stereo-defect distribution and molecular mass in the non-isothermal crystallization behavior of β-nucleated isotactic polypropylene. Soft Mater 14:170–179. https://doi.org/10.1080/1539445X.2016.1176044

30. Kang J, Wang B, Peng H, et al (2014) Investigation on the structure and crystallization behavior of controlled-rheology polypropylene with different stereo-defect distribution. Polym Bull 71:563–579. https://doi.org/10.1007/s00289-013-1077-y

31. Busico V, Cipullo R, Mingione A, Rongo L (2016) Accelerating the Research Approach to Ziegler-Natta Catalysts. Ind Eng Chem Res 55:2686–2695. https://doi.org/10.1021/acs.iecr.6b00092

32. Hendrickson G (2006) Electrostatics and gas phase fluidized bed polymerization reactor wall sheeting. Chem Eng Sci 61:1041–1064. https://doi.org/10.1016/j.ces.2005.07.029

33. Zhang P, Liang C, Zhou Q, et al (2021) Experimental investigation of particle adhesion on the wall due to electrostatic charge in gas-solid fluidized beds. Powder Technol 387:373–384. https://doi.org/10.1016/j.powtec.2021.04.041

34. Reichardt C, Welton T (2011) Solvents and Solvent Effects in Organic Chemistry. Wiley-VCH Verlag GmbH & Co. KGaA